

# Search for direct production of $a_2(1320)$ and $f_2(1270)$ mesons in $e^+e^-$ annihilation

M.N. Achasov, S.E. Baru, K.I. Beloborodov, A.V. Berdyugin,  
A.G. Bogdanchikov, A.V. Bozhenok, D.A. Bukin, S.V. Burdin,  
T.V. Dimova, A.A. Drozdetsky, V.P. Druzhinin,  
M.S. Dubrovin, I.A. Gaponenko, V.B. Golubev,  
V.N. Ivanchenko, A.A. Korol, M.S. Korostelev, S.V. Koshuba,  
G.A. Kukartsev, E.V. Pakhtusova, A.A. Polunin, E.E. Pyata,  
A.A. Salnikov, S.I. Serednyakov, V.A. Sidorov, Z.K. Silagadze,  
A.N. Skrinsky, V.V. Shary, Yu.M. Shatunov, A.V. Vasiljev\*

Budker Institute of Nuclear Physics,  
Novosibirsk State University,  
Lavrentiev Avenue, 11,  
Novosibirsk, 630090, Russia

## Abstract

A search for direct production of C-even resonances  $a_2(1320)$  and  $f_2(1270)$  in  $e^+e^-$  annihilation was performed with SND detector at VEPP-2M  $e^+e^-$  collider. The upper limits of electronic widths of these mesons were obtained at 90 % confidence level:

$$\Gamma(a_2(1320) \rightarrow e^+e^-) < 0.56 \text{ eV},$$

$$\Gamma(f_2(1270) \rightarrow e^+e^-) < 0.11 \text{ eV}.$$

PACS: 13.40.Gp; 13.65.+i; 13.85.Rm; 14.40.Cs

*Keywords:*  $e^+e^-$  collisions; Tensor meson; Detector

---

\*Fax: +7(3832)342163; e-mail: vasiljev@inp.nsk.su

## 1. Introduction

Traditional subject of study in  $e^+e^-$  collisions are vector states with  $J^{PC}=1^{--}$ . Direct production of  $C$ -even mesons ( $J^{PC}=0^{-+}, 0^{++}, 2^{++}, \dots$ ) is also possible via two-photon annihilation (fig.1) although it is suppressed by a factor of  $\sim \alpha^2$  for tensor mesons. Production of scalar and pseudoscalar states is further suppressed by additional 'chirality' factor  $m_e^2/s$ . Nevertheless,  $e^+e^-$  colliding beam technique remains one of the most sensitive methods of measurement of electronic widths of  $C$ -even resonances ( $X$ ) with masses around 1 GeV [1, 2].

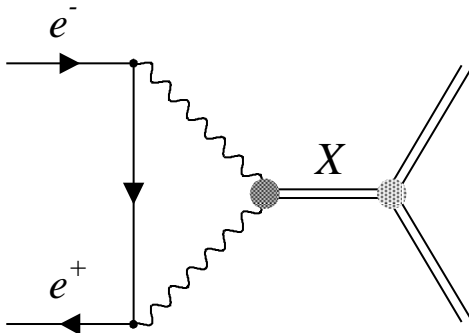


Figure 1: The diagram of direct production of  $C$ -even resonance in  $e^+e^-$  collision.

In the unitarity limit [3] when both virtual photons (fig.1) are on the mass shell the leptonic width is completely determined by imaginary part of the  $X \rightarrow e^+e^-$  transition amplitude which is related to the  $X$  two-photon width [4]. Taking into account both real and imaginary parts of the  $X \rightarrow e^+e^-$  transition amplitude  $Z$ , the branching ratio of  $X \rightarrow e^+e^-$  decay can be written as follows:

$$Br(X \rightarrow e^+e^-) = \frac{2\alpha^2}{9} \cdot Br(X \rightarrow \gamma\gamma) \cdot \left[ 1 + (\text{Re}Z)^2 / (\text{Im}Z)^2 \right] \quad (1)$$

At present only branching ratios of pseudoscalar mesons  $\eta \rightarrow \mu^+\mu^-$  [5] and  $\pi^0 \rightarrow e^+e^-$  [6] are measured with accuracies of 15 % and 8 % respectively.

The energy range of the electron-positron collider VEPP-2M [7] allows to perform a search for production of the lightest tensor mesons  $f_2(1270)$  and  $a_2(1320)$  in  $e^+e^-$  annihilation. Using the experimental values [5] of the two-photon widths of these mesons, one can estimate their electronic widths in the unitarity limit:

$$\Gamma(a_2(1320) \rightarrow e^+e^-)_{ul} \sim 1 \cdot 10^{-2} \text{ eV}, \quad (2)$$

$$\Gamma(f_2(1270) \rightarrow e^+e^-)_{ul} \sim 3 \cdot 10^{-2} \text{ eV} \quad (3)$$

The only experimental attempt to measure these widths was taken in the ND experiment at VEPP-2M collider [8] in the search for the reactions:

$$e^+e^- \rightarrow a_2(1320) \rightarrow \eta\pi^0, \quad (4)$$

$$e^+e^- \rightarrow f_2(1270) \rightarrow \pi^0\pi^0 \quad (5)$$

As a result the following upper limits at 90 % confidence level were obtained:  $\Gamma(a_2(1320) \rightarrow e^+e^-) < 25 \text{ eV}$ ,  $\Gamma(f_2(1270) \rightarrow e^+e^-) < 1.7 \text{ eV}$  [1, 2].

## 2. Detector and experiment

In the present work the search for the reactions (4, 5) was continued. The experiments [9] were carried out in 1997 and 1999 at VEPP-2M  $e^+e^-$  collider with the SND detector [10, 11]. Four successive scans of the energy range  $2E_0=1.04\text{--}1.38 \text{ GeV}$  with the step  $\Delta(2E_0)=0.01 \text{ GeV}$  were performed. The total integrated luminosity of  $9 \text{ pb}^{-1}$  was uniformly distributed over this energy range. For present analysis only the data with  $2E_0$  above 1.15 GeV with an integrated luminosity of  $6.5 \text{ pb}^{-1}$  was used.

The SND detector is a universal nonmagnetic detector. Its main part is a three-layer electromagnetic calorimeter consisted of 1630 NaI(Tl) crystals covering 90 % of  $4\pi$  solid angle. The energy resolution of the calorimeter for photons with energy  $E$  can be described by the function  $\sigma_E/E = 4.2\%/\sqrt[4]{E, \text{ GeV}}$ , the angular resolution is close to  $1.5^\circ$ , the resolution over  $\pi^0$  invariant mass is approximately 8 %. For measurement of charged

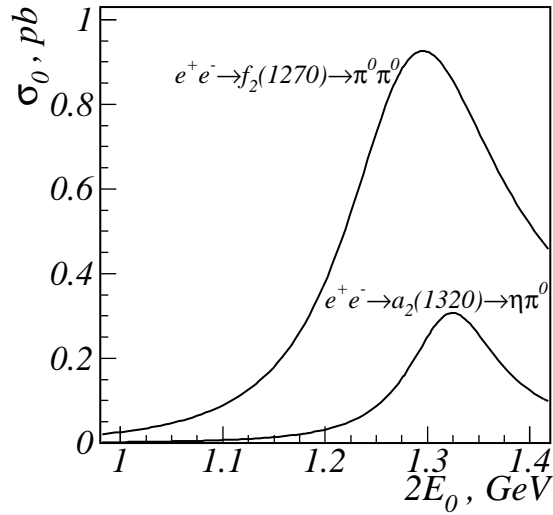


Figure 2: Energy dependences of the cross sections of the reactions  $e^+e^- \rightarrow f_2(1270) \rightarrow \pi^0\pi^0$ ,  $e^+e^- \rightarrow a_2(1320) \rightarrow \eta\pi^0$  calculated in the unitarity limit.

particles directions the system of two central cylindrical drift chambers is used. More detailed description of the SND detector can be found in [11].

A search for the reaction (5) was carried out taking into account the differential cross section calculated in [12]:

$$\frac{d\sigma}{d\Omega} = 12.5 \cdot \left( \frac{\sqrt{s}}{m} \right)^6 \cdot \frac{\Gamma^2 \cdot B_{ee} \cdot B_{\pi^0\pi^0}}{(m^2 - s)^2 + m^2\Gamma^2} \cdot \sin^2(2\theta), \quad (6)$$

where  $s = 4E_0^2$ ;  $m$ ,  $\Gamma$ ,  $B_{ee}$ , and  $B_{\pi^0\pi^0}$  are the  $f_2$ -resonance mass, width, and branching ratios of its decays into  $e^+e^-$  and  $\pi^0\pi^0$ . The cross sections of the reactions (4) and (5), calculated in the unitarity limit, are shown in the fig.2. Expected numbers of events, corresponding the collected luminosity distribution, are 1 and 4 for the reactions (4) and (5) respectively.

### 3. Events selection

For the primary selection of events the following cuts were applied:

*four photons and no charged particles are found in an event;*

*energy deposition in the calorimeter  $E_{tot} > 0.7 \cdot (2 \cdot E_{beam})$ ;*

*total momentum of an event measured by the calorimeter  $P_{tot} < 0.3 \cdot (2 \cdot E_{beam}/c)$ .*

A total of 12.6 thousand events satisfying the above criteria were found.

Main background for the processes (4, 5) comes from the following reactions with a 3 order of magnitude larger cross sections:

$$e^+e^- \rightarrow 4\gamma \text{ (QED)}, \quad (7)$$

$$e^+e^- \rightarrow \omega\pi^0 \rightarrow \pi^0\pi^0\gamma, \quad (8)$$

where the reaction (8) produces events satisfying  $4\gamma$  selection cuts due to merging of close photons or loss of soft photons through openings in the calorimeter.

Other background processes are the reactions with emission of hard photon at large angle by one of the initial particles and subsequent production of  $\rho$ ,  $\omega$ , or  $\phi$  meson:

$$e^+e^- \rightarrow V\gamma \rightarrow \pi^0\gamma\gamma, \eta\gamma\gamma, \quad V = \rho, \omega, \phi \quad (9)$$

Their cross sections are 1–2 orders of magnitude larger than these of the processes under study (4, 5) [13].

Additional background comes from the QED processes:

$$e^+e^- \rightarrow 2\gamma, 3\gamma \quad (10)$$

with detection of additional stray photons of beam background. Energy spectrum and angular distribution of such photons were studied on special class of events with trigger from external generator. Analysis of these events shows that stray photons mainly concentrate at small angles with respect to the beam axis and their spectrum decreases sharply with increase of energy. To suppress a contribution from the processes (10) with extra photons, the following restrictions on angle  $\theta_\gamma$  and energy  $E_\gamma$  of each photon in the event were applied:

$$27^\circ < \theta_\gamma < 153^\circ, \quad E_\gamma > 0.1 \cdot E_{beam}.$$

Although these cuts reduce efficiency for the processes under study (4, 5) by 30 %, they strongly, by about five times, suppress contribution of the QED processes (7, 10). After all above listed cuts 2036 events were selected, which correspond to the total detection cross section  $\sim 0.3$  nb.

To suppress background events with merged photons the special parameter  $\zeta$  [14] was used. This parameter is a measure of likelihood of the hypothesis that given transverse energy deposition profile of a photon cluster in the calorimeter can be attributed to a single photon emitted from the beam interaction point. The requirement

$$\zeta < 0$$

for all photons in an event allows to suppress significantly the contribution of events with merged photons and events of the process

$$e^+e^- \rightarrow K_S K_L \rightarrow \pi^0 \pi^0 K_L \quad (11)$$

with nuclear interaction of  $K_L$ . This cut reduces the number of experimental events by 40 % while the detection efficiencies for the processes (4) and (5) decrease by only 6 % and 4 % respectively.

For the events left, kinematic fit with requirement of energy-momentum conservation was performed and corresponding value of  $\chi^2$  was calculated. For further analysis 842 events with

$$\chi^2 < 20$$

were selected. This number is in a good agreement with expected contribution of the background processes (7 - 9) obtained by simulation. About 65 % of it comes from the process (8).

To suppress contribution of the process (8) the special parameter  $\xi_{\omega\pi^0}$  was constructed taking into account the topology of the process (8) with only four photons detected. Three hypotheses were considered:

- 1) undetected photon is from recoil  $\pi^0$  (12 possible combinations);
- 2) undetected photon is the recoil photon from  $\omega$  decay (6 possible combinations);
- 2) undetected photon comes from  $\pi^0$  in  $\omega$  decay (6 possible combinations).

For all 24 possible combinations of photons the values of

$$\chi_i^2 = \frac{(m_1 - m_\omega)^2}{\sigma_\omega^2} + \frac{(m_2 - m_{\pi^0})^2}{\sigma_{\pi^0}^2} \quad (12)$$

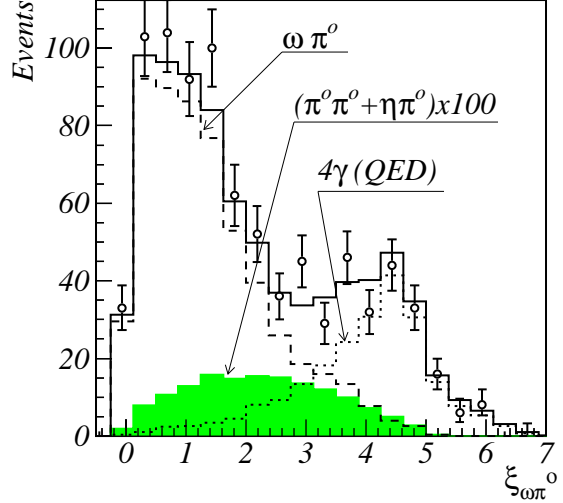


Figure 3: Distribution of 842 experimental events over the parameter  $\xi_{\omega\pi^0}$  (circles with error bars). The clear histogram is the sum of expected contributions of the main background processes (7 - 9), shaded histogram is an expected signal of the processes under study (4, 5) multiplied by 100. Dashed and dotted lines show individual contributions of the main background processes (8) and (7) respectively.

were calculated. Here  $m_1$ , depending on the combination being considered, is either invariant mass of three photons or recoil mass of two photons,  $m_2$  is an invariant mass of two photons for a given combination;  $m_\omega$  and  $m_{\pi^0}$  — the masses of  $\omega$  and  $\pi^0$  mesons respectively. The parameter  $\xi_{\omega\pi^0}$  was defined as

$$\xi_{\omega\pi^0} = \ln(1 + \min_i(\chi_i^2)), \quad i = 1, \dots, 24. \quad (13)$$

It is seen from  $\xi_{\omega\pi^0}$  distributions in the fig.3 that events of the process (8) concentrate in the left side of the plot while processes under study (4, 5) have flatter and wider spectrum allowing the use of this parameter for further cuts.

Similarly to eq. 12,13 the parameters  $\xi_{\eta\pi^0}$ ,  $\xi_{\pi^0\pi^0}$  and  $\xi_{\omega\pi^0\gamma}$ ,  $\xi_{\omega\eta\gamma}$ ,  $\xi_{\phi\eta\gamma}$ ,  $\xi_{\phi\pi^0\gamma}$  for selection of the processes (4), (5) and (9) respectively were constructed.

#### 4. Final events selection and results

To select candidate events of the reaction (5)

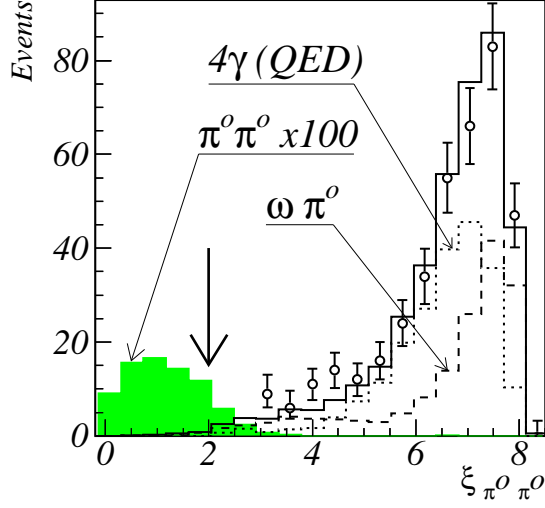


Figure 4: The  $\xi_{\pi^0 \pi^0}$  distributions: circles with error bars — experimental data; clear histogram — expected contribution of the background processes (7 - 9), shaded histogram — expected signal of the process (5) multiplied by 100. In addition the individual contributions of main backgrounds, (8) — dashed line and (7) — dotted line, are shown separately. Arrow shows the cut  $\xi_{\pi^0 \pi^0} < 2$  used for final selection.

the following cuts were imposed:

$$\xi_{\omega \pi^0} > 1.5, \quad \xi_{\omega \pi^0 \gamma} > 2, \quad \xi_{\pi^0 \pi^0} < 2. \quad (14)$$

The  $\xi_{\pi^0 \pi^0}$  distribution before the last cut from (14) is shown in fig. 4. No experimental events passed selection cuts, while 0.7 events of the process under study (5) (in the unitarity limit) and 1.4 events of the background processes are expected from simulation. The selection efficiency for the process (5) is close to 17%.

To search for the reaction (4) the following cuts were applied to 842 experimental events selected above:

$$\xi_{\omega \pi^0} > 2, \quad \xi_{\omega \eta \gamma} > 2, \quad \xi_{\phi \eta \gamma} > 1, \quad \xi_{\eta \pi^0} < 2. \quad (15)$$

The  $\xi_{\eta \pi^0}$  distribution before the last cut from (15) is shown in fig. 5. Here again no experimental events were found. Expected number of events of the process under study (4) is 0.05, the selection efficiency is about 5% taking into account all decay modes of  $\eta$  meson. Calculated contribution of the background processes (7 - 9) is 5.5 events.

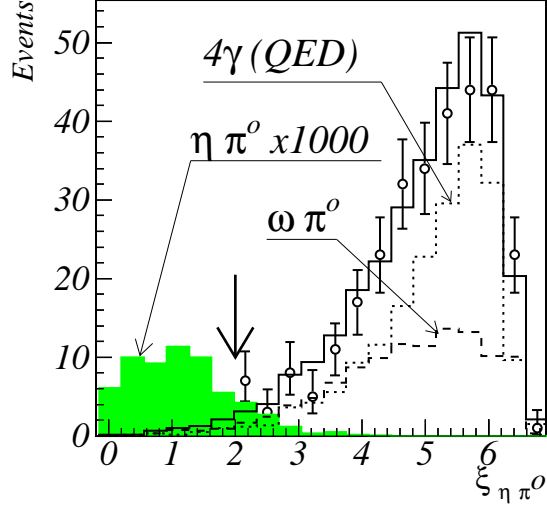


Figure 5: The  $\xi_{\eta \pi^0}$  distributions: circles with error bars — experimental data; clear histogram — expected contribution of the background processes (7 - 9), shaded histogram — expected signal of the process (5) multiplied by a factor 1000. In addition, individual contributions of main backgrounds, (8) — dashed line — and (7) — dotted line, are shown separately. Arrow shows the cut  $\xi_{\eta \pi^0} < 2$  used for final selection.

We used the following formulae to obtain the upper limits of branching ratios of electronic decays of tensor mesons  $T = a_2(1320), f_2(1270)$ :

$$Br(T \rightarrow e^+ e^-) < \frac{k_0}{N_{expt}}. \quad (16)$$

Here  $N_{expt} = \sum \Delta L(E_i) \cdot \sigma(E_i) \cdot (1 + \delta) \cdot \epsilon(E_i)$  is expected number of events of the process under study with  $Br(T \rightarrow e^+ e^-) = 1$ ,  $k_0 = 2.44$  is a 90% CL Poisson limit in case of none experimental events observed ([5], p. 177),  $\Delta L(E_i)$  is an integrated luminosity at the energy  $E_i$ ,  $\sigma(E_i)$  and  $\epsilon(E_i)$  are the cross section and the selection efficiency of the process under study, calculated by MC simulation,  $\delta$  is a radiative correction. In the table (1) upper limits at 90% CL on branching ratios and electronic widths of  $a_2(1320)$  and  $f_2(1270)$  calculated according to eq.(16) as well as

Table 1: The upper limits of branching ratios and electronic widths of tensor mesons  $a_2(1320)$  and  $f_2(1270)$  obtained in this work as compared with current experimental data and theoretical calculations in the unitarity limit [3].

|                                       | this work<br>(SND'2000) | ND'91 [2]<br>(PDG'98 [5]) | calculation in the<br>unitarity limit [3] |
|---------------------------------------|-------------------------|---------------------------|---|
| $Br(a_2 \rightarrow e^+e^-)$          | $< 6 \cdot 10^{-9}$     | $< 2.3 \cdot 10^{-7}$     | $1.1 \cdot 10^{-10}$                      |
| $Br(f_2 \rightarrow e^+e^-)$          | $< 6 \cdot 10^{-10}$    | $< 9 \cdot 10^{-9}$       | $1.6 \cdot 10^{-10}$                      |
| $\Gamma(a_2 \rightarrow e^+e^-)$ , eV | $< 0.56$                | $< 25$                    | 0.012                                     |
| $\Gamma(f_2 \rightarrow e^+e^-)$ , eV | $< 0.11$                | $< 1.7$                   | 0.029                                     |

theoretical predictions are presented.

## 5. Discussion

The upper limits of the  $a_2 \rightarrow e^+e^-$  and  $f_2 \rightarrow e^+e^-$  branching ratios obtained in this work are respectively 45 and 15 times lower than previous experimental values [1]. Our limit for the electronic width of  $f_2(1270)$  is only four times higher than its unitarity limit. It allows for the first time to place a meaningful experimental limit for the ratio of the real and imaginary parts of  $f_2 \rightarrow e^+e^-$  transition amplitude:

$$(\text{Re}Z)^2/(\text{Im}Z)^2 < 2.8 \quad (17)$$

at 90 % confidence level. Unfortunately, we could not find any theoretical estimates for this parameter. To observe the process (5) with SND detector it is necessary to increase integrated luminosity by 1–2 orders of magnitude.

## Acknowledgments

This work is supported in part by Russian Fund for Basic Researches, grants No. 00-02-17481 and 00-15-96802, and STP “Integration” No. 274.

## References

- [1] P.V. Vorobyev et al., Sov. J. Nucl. Phys. 48 (1987) 436.
- [2] S.I. Dolinsky et al., Phys. Rep. 202 (1991) 99.
- [3] A.I. Vainshtein and I.B. Khriplovich, Yad. Fiz. 13 (1971) 620.
- [4] V.N. Novikov and S.I. Eidelman, Sov. J. Nucl. Phys. 21 (1975) 1029.
- [5] Review of Particle Physics, Eur. Phys. J. C 3 (1998).
- [6] E799-II / KTeV Collaboration, Phys. Rev. Lett. 83 (1999) 922, hep-ex/9903007.
- [7] G.M. Tumaikin et al., Proceedings of the 10-th International Conference on High Energy Particle Accelerators, Serpukhov, v.1, 443 (1977).
- [8] V.B. Golubev et al., Nucl. Instr. and Methods 227 (1984), p.467.
- [9] M.N. Achasov et al., Novosibirsk preprint Budker INP 98-65 (1998).
- [10] V.M. Aulchenko et al., SND - Detector for VEPP-2M and Phi-Factory, in: Proc. Workshop on Physics and Detectors for DAFNE (Frascati, April 1991), p.605.
- [11] M.N. Achasov et al., Nucl. Instr. and Meth. A 449 (2000) 125, hep-ex/9909015.
- [12] A.A. Belkov, E.V. Kuraev and V.N. Perushin, Yad. Fiz. 40 (1984) 1483.
- [13] M. Benayoun, S.I. Eidelman, V.N. Ivanchenko and Z.K. Silagadze, Mod. Phys. Lett. A 14, No. 37 (1999) 2605.
- [14] A.V. Bozhenok, V.N. Ivanchenko and Z.K. Silagadze, Nucl. Instr. and Meth. A 379 (1996) 507.
- [15] E.A. Kuraev and V.S. Fadin, Sov. J. Nucl. Phys. 41 (1985) 466.